Check for updates

Markus Keller ORCID iD: 0000-0002-8654-9920

Balasubramaniem Ashokkumar ORCID iD: 0000-0003-2213-5400

Novel *ALDH3A2* mutations in structural and functional domains of FALDH causing diverse clinical phenotypes in Sjögren-Larsson Syndrome patients

Mohan Rajeshwari[1], Sellamuthu Karthi[2], Singh Reetu[1], Stephanie Efthymiou[3], Vykuntaraju K Gowda[4], Perumal Varalakshmi[1], Varunvenkat M Srinivasan[4], Henry Houlden[3], Markus A Keller[5], William B Rizzo[6], and Balasubramaniem Ashokkumar[1*]

1. School of Biotechnology, Madurai Kamaraj University, Madurai, INDIA
2. Department of Biochemistry & Molecular Biology, Sealy Center for Molecular Medicine, UTMB
3. Department of Molecular Neuroscience and Neurogenetics Laboratory, UCL Institute of Neurology, London, UK
4. Department of Pediatric Neurology, Indira Gandhi Institute of Child Health, Bangalore, INDIA
5. Human Genetics Section, Medical University of Innsbruck, Innsbruck, Austria
6. Division of Inherited Metabolic Diseases, University of Nebraska Medical Center, Omaha, Nebraska, USA

*Correspondence to: Balasubramaniem Ashokkumar, Department of Genetic Engineering, School of Biotechnology, Madurai Kamaraj University, Madurai - 625 021, India.

E-mail: rbashokkumar@yahoo.com

Author ORCID iDs:

Mohan Rajeshwari: 0000-0002-3832-5711, Sellamuthu Karthi: 0000-0002-5703-9462, Singh Reetu: 0000-0001-5896-656X, Stephanie Efthymiou: 0000-0003-4900-9877, Vykuntaraju K Gowda: 0000-0001-7244-0492, Perumal Varalakshmi: 0000-

This article has been accepted for publication and undergone full peer review but has not been through the copyediting, typesetting, pagination and proofreading process, which may lead to differences between this version and the Version of Record. Please cite this article as doi: 10.1002/humu.24236.

This article is protected by copyright. All rights reserved.

Accepted Article

0002-5420-4688, Varunvenkat M Srinivasan: 0000-0003-3892-4439, Henry Houlden: 0000-0002-2866-7777, Markus A Keller: 0000-0002-8654-9920, William B Rizzo: 0000-0002-3686-0518, Balasubramaniem Ashokkumar: 0000-0003-2213-5400.

ABSTRACT

Mutations in *ALDH3A2* cause Sjögren-Larsson Syndrome (SLS), a neuro-ichthyotic condition that is caused by deficiency of fatty aldehyde dehydrogenase (FALDH). We screened for novel mutations causing SLS among Indian ethnicity, characterized the identified mutations *in silico* and *in vitro*; and retrospectively evaluated their role in phenotypic heterogeneity. Interestingly, asymmetric distribution of non-classical traits was observed in our cases. Nerve conduction studies suggested intrinsic-minus-claw hands in two siblings, a novel neurological phenotype to SLS. Genetic testing revealed 5 novel homozygous *ALDH3A2* mutations in six cases: Case-1-NM_000382.2:c.50C>A, NP_000373.1:p.(Ser17Ter); Case-2-NM_000382.2:c.199G>T, NP_000373.1:p.(Glu67Ter); Case-3-NM_000382.2:c.1208G>A, NP_000373.1:p.(Gly403Asp); Case-4-NM_000382.2:c.1325C>T, NP_000373.1:p.(Pro442Leu); Case-5&6-NM_000382.2:c.1349G>A, NP_000373.1:p.(Trp450Ter). The mutations identified were predicted to be pathogenic and disrupts the functional domains of the FALDH. p.(Pro442Leu) at the C-terminal α-helix, might impair substrate gating process. Mammalian expression studies with exon-9 mutants confirmed the profound reduction in the enzyme activity. Diminished aldehyde oxidizing activity was observed with cases-2&3. Cases-2 & 3 showed epidermal hyperplasia with mild intracellular edema, spongiosis, hypergranulosis, and perivascular-interstitial lymphocytic infiltrate and a leaky eosinophilic epidermis. The presence of keratin-milia like lipid vacuoles implies defective lamellar secretion with p.(Gly403Asp). This study improves our understanding of the clinical and mutational diversity in

This article is protected by copyright. All rights reserved.

Accepted Article

SLS, which might help to fast-track diagnostic and therapeutic interventions of this debilitating disorder.

Graphical Abstract

Functional characterization of novel ALDH3A2 mutations from Indian ethnicity

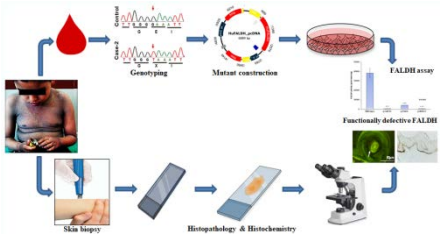

Keywords: FALDH, Sjögren -Larsson Syndrome, *ALDH3A2*, Ichthyosis, Neuro-cutaneous, Exome sequencing

Introduction

Sjögren-Larsson syndrome (MIM# 270200), an autosomal recessive neurocutaneous disorder with early childhood onset, is primarily caused by a defective microsomal fatty aldehyde dehydrogenase. Deficiency of FALDH results in abnormal long chain aldehyde metabolism accumulating fatty alcohols, which leads to clinical features of ichthyosis, intellectual disability, spastic diplegia, leukoencephalopathy and a distinctive retinopathy (Sjögren et al., 1957; Rizzo, 2007). In humans, *ALDH3A2* is on 17p11.2 and spans about 11 exons (Rizzo et al., 1999). Alternative splicing generates two protein isoforms of FALDH in humans (Rogers et al., 1997); a less abundant isoform-1 (NP_001026976.1) in peroxisomes consisting of 508 amino acid residues, whereas isoform-2 (NP_000373.1) in endoplasmic reticulum consists of 485 residues with a different carboxy terminus. Both the FALDH isoforms irreversibly oxidize long-chain fatty aldehydes, fatty alcohols and have a substrate preference for longer ones over shorter ones. SLS skin type secretes premature lamellar body,

This article is protected by copyright. All rights reserved.

Accepted Article

Accepted Article

causing defective stratum corneum membranes, increased trans-epidermal water loss and clinical ichthyosis (Rizzo et al., 2010; Rizzo et al., 1988). Spastic diplegia with white matter abnormalities, pruritus, short stature, epilepsy, macular degeneration and dysarthria are the other presenting symptoms in SLS (Bindu, 2020).

FALDH is a membrane associated homo-oligomeric NAD^+-dependent enzyme, which is composed of three subdomains including a cofactor-binding domain, a catalytic domain and an oligomerization domain (Marchitti, 2010). In FALDH, the residues Leu464 to Val480 constitutes the transmembrane domain, and the so called "gate-keeper helix" core hydrophobic region spans from Ser446 to Leu456 and confers specificity to the substrate cavity and helps in efficient transit of substrate from the membrane surface to the catalytic site (Keller et al., 2014). Interestingly, the exon-9 harbours most of the oligomerization domain residues, catalytic domain residues, as well as the gatekeeper helix residues. Majority of disease-causing mutations are known to impair the catalytic and cofactor domains of FALDH (Weustenfeld et al., 2019). Mutations in any of these vital structural components most likely impacts the stability of the protein, thus making it metabolically defective and leading to accumulation of unprocessed aldehydes.

More than 130 mutations in *ALDH3A2* have been diagnosed to cause SLS so far (http://www.hgmd.cf.ac.uk). In addition to the classical benchmark triad symptoms of SLS, a spectrum of diverse phenotypes is reported among SLS cohorts from various ethnicities from different parts of the world, which is attributed to both genetic variations and epigenetic factors. SLS was first described in Sweden and is reported to have originated at least 600 years ago (Maia, 1974), later it became prevalent among Europe, Middle East, USA, Africa and also in Asian countries like Japan and India. Nearly 48 different neuro-ichthyotic symptoms or phenotypes are

This article is protected by copyright. All rights reserved.

Accepted Article

associated with variations in *ALDH3A2* according to the Human Phenome Ontology database. The cutaneous manifestations in SLS outplay the neurological ones conferring diversity in patients across the world. The heterogeneity of SLS phenome is well documented in an open-access database (www.LOVD.nl/ALDH3A2) by two of our authors upon merging patient-centered literature data of about 178 individuals with 90 different genetic variations reported globally (Weustenfeld et al., 2019). The key factors responsible for such heterogeneity remain elusive. Correlating the phenotypes to their respective genotypes might serve as a promising approach towards unravelling this mystery. In this study, we have profiled the pathogenicity of five novel *ALDH3A2* mutations associated with SLS cases among Indian ethnicity and described their clinical features, which add to understanding the heterogeneity of this intriguing disorder.

Materials and Methods

Study subjects

Six patients with neuro-ichthyotic symptoms descending from five unrelated families of Indian ethnicity were enrolled in this study. We obtained a printed informed consent from parents/guardians of all the participants. All the patients were clinically diagnosed initially, and then mutational analyses were performed. For this, peripheral blood samples were obtained from the six cases, who presented with the major classical SLS traits such as ichthyosis, spasticity and intellectual disability. Cases 5 & 6 are siblings and the remaining 4 probands are unrelated. The healthy control subject is an unrelated and non-SLS individual. This research involving the mammalian expression studies and tissue pathological analysis were monitored, approved and reviewed periodically by the Institutional Ethical Review Board. Detailed clinical

This article is protected by copyright. All rights reserved.

Accepted Article

records of medical history and scientific examinations were recorded and maintained by the hospital.

Isolation of blood genomic DNA

Genomic DNA was scored from the peripheral blood samples of the study subjects using the non-enzymatic method of salting out and purified using Blood genomic DNA purification kit (Hi-Media, India). Integrity of the DNA obtained was also ensured with an agarose gel electrophoresis before subjecting to sequencing. Approximately, 100 ng of DNA so obtained was used as the template for each reaction.

Exome sequencing analysis

Exome Sequencing and annotation was performed for a batch of four cases (case-3, 4, 5 and 6) along with an unaffected carrier mother of case-4 and 5 to compare and rule out the non-pathogenic variants. For this, a library ligated with an adapter was prepared with the SureSelectXT Paired-End Target Enrichment System Sample Prep kit V1 (Agilent Technologies, USA) and the captured libraries were sequenced using a single flow cell lane per sample to mean >80-100X coverage for paired-end reads of 100-bp using HiSeq. 3000 (Illumina Inc., San Diego, CA) according to the manufacturer's instructions. Whole exome data processing and analysis was accomplished using a computational pipeline following the general Human Genome Project workflow. The raw reads alignment was based on UCSC hg 19. Following the recalibration of the base quality and local realignment, the resulting calls were annotated with Variant Effect Predictor.

This article is protected by copyright. All rights reserved.

Accepted Article

Exon specific PCR and sequencing

The rest of the cases were analysed using traditional exon-wise screening for mutations by PCR amplification followed by Sanger sequencing. *ALDH3A2* exons were amplified using 10 pmol of the exon specific primer sets, which are designed to amplify the exon-intron boundaries (Supplementary Table S1) with a PCR mix containing 1.0 Unit of Taq polymerase and 10 mM dNTPs under the following PCR conditions: (i) Touchdown (TD-PCR) for all the exons except exon-4 and exon-10: Initial denaturation at 94^{o}C for 5 min; 10 subsequent amplification cycles performed at 94^{o}C for 40 sec, 65^{o}C for 50 sec and 72^{o}C for 2 min; followed by 20 subsequent cycles performed at 94^{o}C for 40 sec, 55^{o}C for 50 sec and 72^{o}C for 2 min and a final extension at 72^{o}C for 10 min. (ii) For exon-4 and exon-10 the PCR reaction was performed with the following conditions: Initial denaturation at 94^{o}C for 5 min; 35 subsequent amplification cycles performed at 94^{o}C for 40 sec, 43.5^{o}C (for exon-4)/55^{o}C (for exon-10) for 50 sec and 72^{o}C for 2 min. The PCR products were gel purified using FavorPrepTM Gel/PCR purification kit (Favorgen, Taiwan) and sequenced bidirectionally using BigDye Terminator Reaction Chemistry v3.1 on Applied Biosystems 3730 DNA analyzers (Applied Biosystems, Carlsbad, USA). The electropherograms so obtained were analysed with Chromas 2.6.6 software to identify disease associated sequence variants of *ALDH3A2* causing SLS. Mutations were screened by comparing to the wild-type sequences of *ALDH3A2* (NCBI accession: NM_000382.3) and were designated using the cDNA numbering system.

Clinical and mutational profiling

In order to profile the heterogenic clinical manifestations in SLS probands, the edgotype datasheet was generated for all the 6 SLS cases enrolled in this study.

This article is protected by copyright. All rights reserved.

Accepted Article

Nearly 23 phenotypes corresponding to SLS were categorized into six subclasses as (i) Developmental; (ii) Neurological; (iii) Behavioural; (iv) Muscular; (v) Ichthyotic and (vi) other rare phenotypes. Genotypic information corresponding to the *ALDH3A2* mutation positive cases was also supplemented to make it a holistic edgotype datasheet.

In silico **analysis**

The pathogenicity of the novel mutations discovered in this study was predicted using various online tools such as Mutation Taster, MutPred2, PROVEAN, DynaMut server and PredictSNP. The functional impact of the novel mutations was also assessed at the mRNA level using RNAfold server. At the protein level, change in vibrational entropy, increase/decrease in structural flexibility and dynamics in the mutants was predicted using DynaMut server and depicted as surface structures of 4QGK model (obtained from PDB) with different colour codes. Theoretical models of both the catalytic domain and the C-terminal oligomerization domain of FALDH were generated using UCSF chimera interface to modeller based on the comparative homology modelling strategy with 4QGK as a template to check for changes in the conformation. Missense mutations were introduced using UCSF chimera with rotamers from Dunbrack 2010 rotamer library (Shapovalov and Dunbrak 2011). The Mutabind2 tool predicted the impact of these missense mutations on proteostasis of the FALDH protein. Transmembrane region (Lys461-Tyr485) of FALDH was modelled separately using I-TASSER module and joined to the 4QGK using standard peptide bond criteria in UCSF chimera. The changes in hydrophobicity of the C-Terminal oligomerization domain (Ser420-Asn443) were depicted as surface structures of the full-length FALDH molecule (485 residues) with/without missense mutations using UCSF chimera. The displacement of membrane orientation of the

This article is protected by copyright. All rights reserved.

Accepted Article

protein due to missense mutations was predicted with the FALDH/membrane complex generated using CHARMM-GUI membrane builder server. The membrane composition was assigned so as to mimic the membranous environment of endoplasmic reticulum.

PCR/RFLP analysis

DNA sequence analysis using NEB cutter online tool (New England Biolabs, USA) for predicting changes in the restriction sites revealed an additional target for *Hinf*I enzyme due to c.1208G>A mutation in exon-9 of *ALDH3A2* gene. This predicted outcome was confirmed by RFLP analysis with *Hinf*I enzyme digestion of exon-specific PCR products for probands and both parents and healthy controls to confirm the pattern of inheritance of the mutant allele.

Site directed mutagenesis

Three mutant constructs of *ALDH3A2* having mutations c.1208G>A or c.1325C>T or c.1349G>A were generated by *Dpn*I method (Zheng et al., 2004) using pcDNA-3.1(+)-FALDH vector as the template with specific mutant primer sets (Supplementary Table S1). Following the PCR, amplicons were digested with *Dpn*I (Thermo Scientific, USA) for 3 h at 37 °C to remove the methylated templates, and a 10 µl aliquot of gel-purified products were transformed into *E. coli* DH5α. The mutations generated in the variant *ALDH3A2* constructs were sequence verified before further analysis.

Cell culture and transfection

FALDH-deficient Chinese hamster ovary cells (CHO-K1A) were maintained in F12 medium with 10% Fetal Calf Serum and 100,000 U/L penicillin, and 10 mg/L

This article is protected by copyright. All rights reserved.

Accepted Article

streptomycin. To determine FALDH activity, cells at 80-90% confluency (~100000 cells/well in 6-well plate) were transfected with 3 μg of the wild-type (pcDNA-3.1(+)-FALDH) and mutant constructs of *ALDH3A2* (c.1208G>A or c.1325C>T or c.1349G>A in pcDNA-3.1(+)-FALDH) with 3 μl of Lipofectamine 2000 (Invitrogen Life Technologies, CA). Cells were then harvested after 24 h for FALDH assay.

FALDH activity assay

FALDH activity by cells transfected with wild-type and mutant *ALDH3A2* constructs was measured using octadecanal (Rizzo et al., 1991). Octadecanal was chemically synthesized from octadecanol using chromium oxide as catalyst and purified to 97% using thin layer chromatography (Kelson et al., 1997). FALDH enzyme activity was measured as the octadecanal-dependent production of fluorescent NADH from non-fluorescent NAD^+ using a 96-well microplate fluorometer (SpectraMax Gemini XS, Molecular Devices). Assay was performed in triplicate with 300 μl of reaction mixture containing Tris-HCl (50 mM), pH 9.5, 0.1%Triton X-100, β-NAD^+ (1.5 mM), bovine serum albumin (0.5 mg/ml), pyrazole (10 mM), octadecanal (160 mM), and 10-20 μg cell homogenate and then, mixture was incubated at 37° C for 30 minutes. NADH production was then monitored using an excitation wavelength of 340 nm and the emission wavelength of about 455 nm. Cell homogenate protein content was determined (Lowry et al., 1951) and FALDH enzyme activity was recorded in pmol of octadecanal oxidized/min/mg protein.

Histopathology

In order to substantiate the cutaneous pathogenesis of the *ALDH3A2* variants in SLS, punch biopsies of the skin (4 mm) were collected from the rectus femoris region of leg of each patient with 1% lignocaine as local anaesthesia and the tissues were snap

This article is protected by copyright. All rights reserved.

Accepted Article

frozen in liquid nitrogen and maintained in dry ice until sectioned. Tissues were mounted on individual cryostat chucks with the help of cryostat freezing medium and frozen for 45 min at -29 °C inside the cryostat machine (Leica Biosystems, Nussloch GmbH, Germany). 12 µM cryostat sections were prepared and mounted on slides, which were then fixed with 95% ethanol for 45 min. After a wash, the slides were first treated with Hematoxylin (H) solution followed by a quick dip in Lithium carbonate solution. After removing the residual stain with distilled water, slides were counter stained with Eosin (E) for 10 sec followed by a 95% ethanol wash. After fixation with 100% ethanol and xylene, the slides were mounted with DPX mountant using a coverslip. This experiment was performed in triplicate. The fluorescing nature of eosin was utilized for better describing the dermatological features with fluorescent microscopy (Olympus, USA). The excitation wavelength was 534 nm and the emission wavelength was 544 nm. The H&E slides were reviewed by experienced pathologists who were blinded about the study details.

Histochemistry

Aldehyde oxidizing activity was detected by histochemical staining of frozen tissue sections (Rizzo et al., 2010). 12 µM cryostat sections were prepared as mentioned for histopathological studies in glass slides. Slides were then incubated at 37°C for 90 min in 50 mM Tris-HCl buffer (pH-8.5); 3.0 mM NAD; 16 mM cobaltous chloride; 0.33 mg/ml MTT and 8.0 mM octanal. Sections were examined by light microscopy and photographed. After 1-3 h, slides were rinsed twice in water for 5 min each and mounted in glycerin. Slides were examined at 40X and 100X with phase contrast microscopy (Lawrence & Mayo, India) and fluorescence microscopy (Olympus Life Science, Japan).

This article is protected by copyright. All rights reserved.

Accepted Article

Statistical analysis

FALDH activity assay was performed in triplicate and the data is expressed as the mean ± S.E. Statistical analysis was performed using one-way ANOVA followed by Tukey's honest significant difference (HSD) test, with statistical significance set at 0.05 ($P< 0.05$).

Results

We investigated 6 SLS patients comprised of 2 males and 4 females descended from 5 families of Indian ethnicity (Figure 1). The demographic information of the study subjects and the overall clinical manifestations of the cases are summarized in Table 1. The clinical records of the individuals with SLS were analysed, wherein the severity of neurocutaneous manifestations was not related to age. The onset of the SLS symptoms was by birth, but the clinical severity of phenotypes is usually observed around 1-16 years (mean 8 years). Parental consanguinity was noticed in all the 5 families studied. Among them, 5 out of 6 probands (~83%) were preterm by birth. All probands expressed dermatological and neurological phenotypes that correspond to SLS, but the severity varied. All the 6 patients showed ichthyosis (HP:0008064), which was found most prominently over the arm region, palms and soles. All 6 cases exhibited global developmental delay (HP:0001263), and almost all presented with spasticity (HP:0001257) (diplegia-67%; quadriparesis-33%). 67% of them are collodion babies at birth and 16% are presented with periventricular pits on skin (Table 1). Seizure, epilepsy and hyper-intensive skin lesion was observed only in

This article is protected by copyright. All rights reserved.

Accepted Article

case-3. Periventricular white matter changes were observed in about 50% of the cases. Spastic diplegia or spastic quadriparesis was recorded in all the patients. Electroencephalogram (EEG) of case-3 showed multifocal spikes that marked with potentiation of epileptic discharges. All of our patients were non-ambulatory or walked using crutches only. Intellectual disability and cognitive deficits were scored based on various scales of intellectual functioning and adaptive behaviour adapted for Indian population, such as Stanford-Binet Intelligence scale test, Senguin form board test, Bhatia's battery of performance tests of intelligence and Wechsler's intelligence scale for children. The probands expressed severe to moderate intellectual disability. The median IQ of the 6 patients included in this study was 45 (range: 30-70). Case-4 had autism and hyperactivity, which was not seen in the others. 83% (5 out of 6) of the cohort had inability in speaking meaningful words. Other rare phenotypes such as low set ears, microcephaly, alopecia, respiratory distress, hypertelorism, end-gaze nystagmus and presence of small tragus was observed with 16% of the cases. To our surprise, two of the siblings (case-5 and case-6) from the same kindred expressed intrinsic-minus-claw hands (HP:0001171), which is a novel phenotype that has not been reported before among SLS cohorts. Both of them failed the Froment's sign test, a physical examination to show the loss of pinch grip. Nerve conduction studies indicate an axonal sensory and motor neuropathy in lower and upper limbs and hence, they are proven to be intrinsic-minus. Though macular and retinal acuities are pathognomonic feature for SLS, none of our patients expressed ocular manifestations.

Mutational screening of our probands by WES and exon-specific sequencing of *ALDH3A2* gene identified disease associated variants in all of them. These variants included five novel *ALDH3A2* mutations from six SLS probands: (i) case-1, a stop-gain mutation NM_000382.2:c.50C>A, NP_000373.1:p.(Ser17Ter) in exon-1; (ii)

This article is protected by copyright. All rights reserved.

Accepted Article

case-2, a stop-gain mutation NM_000382.2:c.199G>T, NP_000373.1:p.(Glu67Ter) in exon-2; (iii) case-3, a missense mutation NM_000382.2:c.1208G>A, NP_000373.1:p.(Gly403Asp) in exon-9; (iv) case-4, a missense mutation NM_000382.2:c.1325C>T, NP_000373.1:p.(Pro442Leu) in exon-9 and (v) case-5 and case-6 (siblings), a stop-gain mutation NM_000382.2:c.1349G>A, NP_000373.1:p.(Trp450Ter) in exon-9 abolishing gate-keeper helix domain. All of the five *ALDH3A2* variants detected from six probands were found in homozygous state only (Figure 2a). Carrier testing showed that each parent of respective to the SLS probands were heterozygous confirming the recessive mode of inheritance of the disorder, except for cases-5 and 6, wherein mother was heterozygous and father was not available for genotyping. The identified variants were neither listed in the Exome Variant Server (http://evs.gs.washington.edu/EVS/) nor in the 1000 Genomes project database (http://www.1000genomes.org/) or in the dbSNP (build153), thus identifying them as extremely rare and highly likely disease-causing mutations for SLS disease pathology among the patients from Indian ethnicity. Of note, the affected individuals can be distinguished by their phenotypes and the identified *ALDH3A2* variants (Table 1). The stop-gain mutations p.(Ser17Ter) and p.(Glu67Ter) detected from the cases-1 and -2, respectively were found to be located in the NAD-binding domain, resulting in premature truncation of FALDH (Figure 2b). The missense mutations p.(Gly403Asp) and p.(Pro442Leu) identified in the cases-3 and -4 were predicted to be present in the catalytic and oligomerization domain of FALDH, respectively. Likewise, another stop-gain mutation p.(Trp450Ter) recorded in the siblings (case-5 and -6) leads to premature truncation of FALDH, which is devoid of gatekeeper helix domain (Figure 2b). The clinical variant c.1208G>A in the exon-9 of *ALDH3A2* in the case-3 had introduced a target site for *Hinf*1 restriction enzyme. Subsequently, RFLP analysis

This article is protected by copyright. All rights reserved.

Accepted Article

was performed to validate the homozygous state in the proband, whereas all other family members were heterozygous, which is consistent with the autosomal recessive pattern of inheritance in SLS (Supp. Figure S1).

All the novel sequence variants identified in this study were predicted to be pathogenic with c.50C>A, p.(Ser17Ter) being highly deleterious among the three stop-gain mutations (Table 2). Human Splice Finder online tool analysis revealed that all three stop-gain mutations were predicted to potentially alter splicing either by activating exonic cryptic acceptor site with p.(Ser17Ter) or donor site with p.(Glu67Ter) and by introducing an exonic splicing silencer site with p.(Trp450Ter) (Supp. Figure S2). Upon investigating the impact of *ALDH3A2* mutations discovered in this study at the mRNA level with RNAfold server, it was found that the secondary structure becomes misfolded in all the mutants implying a decreased stability (Supp. Figure S3). The transmembrane domain spanning the bilipid layer that stands vital for transit of molecules in and out was found displaced for p.(Pro442Leu) with an increase in $\Delta G_{transfer}$ by 1.2 kcal/mol, tilt angle by 1±1° and a decrease in hydrophobic thickness of the membrane by 1.2±0.5 Å (Figure 3a), which might hamper the function of FALDH enzyme. DynaMut server was used to validate the functional consequences of FALDH variants p.(Gly403Asp) and p.(Pro442Leu), which analyses the stability and dynamics of protein from the changes in conformational entropy. Change in vibrational entropy energy (ΔΔSVib ENCoM) between the wild-type and p.(Pro442Leu) was 1.426 kcal mol^{-1} K^{-1}, with a destabilizing ΔΔG ENCoM of -1.141 kcal/mol and a ΔΔG mCSM of -0.285 kcal/mol, implying gain of molecular flexibility. Whereas, ΔΔSVib ENCoM of p.(Gly403Asp) was -0.407 kcal mol^{-1} K^{-1} with a destabilizing ΔΔG ENCoM of 0.326 kcal/mol and a ΔΔG mCSM of -0.282 kcal/mol, implying diminished molecular flexibility and rigidity of the C-terminal α-

This article is protected by copyright. All rights reserved.

Accepted Article

helix tail. These results show that p.(Gly403Asp) and p.(Pro442Leu) might alter the hydrogen bond network, thereby affecting the conformational flexibility of the C-termini, which is essential for allosteric regulation and conformational gating of FALDH (Figure 3b).

Mutant constructs of *ALDH3A2* with pathogenic novel mutations in the exon-9 of *ALDH3A2* (p.Gly403Asp)/ p.(Pro442Leu) / p.(Trp450Ter) were generated by cloning into pcDNA3.1(+) and expressed in CHO-K1 cells. FALDH activity was measured in cell homogenates. All the mutant constructs showed a significant (P<0.01) decrease in the activity of FALDH enzyme compared to wild-type: p.(Trp450Ter) (98.20%) > p.(Gly403Asp) (98.18%) > p.(Pro442Leu) (88.6%), which clearly demonstrated the destructive nature of the mutations (Figure 4). Missense mutations like p.(Pro442Leu) occurring in the oligomerization domain of the FALDH protein, might also cause SLS by reducing the threshold for spontaneous oligomerization. Likewise, stop-gain variants like p.(Trp450Ter) in the C-terminal gatekeeper helix might produce a functionally deficient FALDH enzyme whose catalytic site might become inaccessible to long-chain fatty aldehydes.

Light microscopic imaging of H&E stained skin sections showed epidermal hyperplasia, mild intracellular edema spongiosis, hypergranulosis and perivascular to interstitial infiltrate in case-3, who harboured c.1208G>A, p.(Gly403Asp) mutation in *ALDH3A2*. Likewise, case-2 with the clinical mutation c.199G>T, p.(Glu67Ter) was presented with epidermal hyperplasia, in addition to higher degree spongiosis and hyperkeratosis (Figure 5). Denser and more compact stratum corneum was observed in both the cases, which revealed that skin had attempted to re-establish the epidermal water barrier. The fluorescence microscopic analysis of the tissue sections revealed eosinophilic leaky epidermis in both the cases-2 and -3. Interestingly, keratin

This article is protected by copyright. All rights reserved.

Accepted Article

containing milia like lipid vacuoles were observed in both the cases encompassing a fluorescent core region, which is different from a hair follicle (Figure 5a). The molecular aetiology behind such cutaneous anomalies requires further investigations.

Fatty aldehyde dehydrogenase activity of skin by histochemical staining using octanal as a substrate has been visualized, wherein the intensity of the enzyme catalysed reaction is proportionate to the quantity of enzyme and length of incubation. Histochemical staining of frozen skin sections from the SLS case harbouring p.(Glu67Ter) mutation for fatty aldehyde oxidizing activity evidenced a profound decrease or absence of staining in the epidermis, while in the case with p.(Gly403Asp) exhibited noticeable changes throughout the epidermis and dermis compared with the skin of healthy control (Figure 5b). The decreasing order of the aldehyde oxidizing activity was p.(Glu67Ter) < p.(Gly403Asp) < healthy control, which strongly substantiated the functionally defective FALDH.

Discussion

Sjögren-Larsson syndrome is one example among the spectrum of neuro-ichthyotic diseases, which comprise a heterogeneous and diverse array of phenotypes, reported in different ethnicities across the world. To date, nearly 130 *ALDH3A2* mutations have been reported to cause SLS worldwide with Sweden being the geographical hotspot with a large number of cases due to a founder effect (Jagell and Liden 1982). There have been 35 clinically diagnosed SLS cases reported with Indian ethnicity, however only three disease-associated mutations in *ALDH3A2* have been documented in three cases (Sakai et al., 2010; Nagappa et al., 2017). Although the 35 cases reported so far in India have a vast clinical diversity (Supp. Table S2) genotype-phenotype correlation have not been performed systematically, and all three mutations

This article is protected by copyright. All rights reserved.

Accepted Article

identified so far have been carried by one or two cases within a single family. This necessitates the need of exome level genetic diagnosis of more SLS patients with Indian ethnicity, which could enhance our understanding about the role of associated genes and environmental factors ensuing to phenotypic variability. We identified and characterized 6 SLS probands from 5 unrelated families of Indian origin. Among them, all exhibited global developmental delay (GDD), spastic quadriparesis or diplegia and ichthyosis. These probands displayed delayed milestones in developmental characteristics such as, speech, cognitive skills, motor skills and social development, mostly before 5 years of age. It is noteworthy to mention that, about 51.4% of the SLS cases reported previously from the Indian ethnicity exhibited delayed developmental milestones in development (Supp. Figure S4), while GDD was observed only in 14% of them. Though GDD is common with genetic disorders such as autism spectrum disorder, fragile X syndrome, cerebral palsy, etc., children with GDD cannot outgrow, but can progress in development with certain therapies (Flore and Milunsky 2012). Except case-3, all other cases exhibited pseudobulbar dysarthria, which is associated with delay of speech and cognitive impairments. It is generally known that impairment of speech and communication is a quite common and important clinical phenotype of SLS (Fuijkschot et al., 2009). Nevertheless, only 11% of the SLS cases expressed dysarthria among previously reported ones from India. Most of the cases were preterm by birth, proving SLS to be a model disease to study preterm birth as reported earlier (Willemsen et al., 1999).

To our surprise, two siblings from the same kindred with c.1349G>A, p.(Trp450Ter) expressed intrinsic-minus-claw hands has been documented as a novel phenotype among SLS cases for the first time in this study. To the best of knowledge, intrinsic-minus-claw hands have not been observed before in any of the SLS patients

This article is protected by copyright. All rights reserved.

Accepted Article

across the world from any ethnic origin. The intrinsic minus claw feature generally occurs due to paralysis of the lumbrical and the interrosei muscles of the hand due to hyperextension of the flexion of proximal-intra-phalangeal joints and metacarpophalangeal joints (Mulder and Landsmeer 1968). We cannot rule out the possibility that this unusual phenotype is due to other genetic or environmental causes in our SLS patients. Except case-3, none of our patients expressed epileptic seizures. Likewise, none of the SLS cases reported previously from India exhibited epileptic seizures. Skin symptoms in our patients include generalized ichthyosis along with a mild pruritus, which is defined as a prime characteristic phenotype of SLS. Nearly 85.7% of the Indian SLS cases reported earlier exhibited generalized ichthyosis, but, only 11.4% of them showed pruritus (Supp. Figure S4). Ichthyosis mainly occurs due to disruption of epidermal water barrier in skin (Roy et al., 2016). The other skin symptom predominantly observed among SLS cases is a collodion membrane at birth. Collodion membrane is found to shed later exposing the underlying layer of skin. History of collodion membrane at birth is less frequently reported with SLS patients across the world. It is very rarely observed (8%) even in the cases previously reported with Indian ethnicity. Remarkably, all of our patients were collodion babies by birth in this study except case-1. Ocular abnormalities are quite common in SLS, with the incidence of macular parafoveal glistening dots reported in 25.7% of cases from Indian ethnicity. To our surprise, none of the cases in our study expressed such ocular abnormalities, although case-1 and case-2 were possibly still too young to develop glistening dots which can first appear later in childhood. Case-1 showed mild end-point gaze evoked nystagmus.

In order to enhance our understanding about the underlying molecular mechanisms of these diverse clinical pathologies, mutational screening and functional

This article is protected by copyright. All rights reserved.

Accepted Article

analysis among SLS cases from Indian ethnicity was performed. Mutational screening of our six probands revealed five novel mutations in *ALDH3A2* gene. In concordance with the autosomal recessive inheritance pattern, all of the *ALDH3A2* variants were found to be homozygous in all six patients, whereas their parents were heterozygous. Three novel mutations identified in this study p.(Gly403Asp), p.(Pro442Leu) and p.(Trp450Ter) are in exon-9 of *ALDH3A2* gene, which spans about 236 bp in length and encodes a 78-residue domain (Gly403 to Lys481). This domain embodies the C-termini of FALDH, and contributes residues to the catalytic domain (Gly209-Phe419); residues of the oligomerization domain (Ser420-Asn443); and more importantly the residues of the gatekeeper helix domain (Ser446-Leu456). These residues confer functional properties to FALDH, especially the C-terminal gate-keeper residues, which are crucial for substrate specificity by facilitating the transit of medium- and long-chain fatty aldehydes between the membrane surface and catalytic site for its oxidation (Keller et al., 2014). According to HGMD database, to date there are 21 mutations reported so far in the amino acid residues encompassing the catalytic domain of the FALDH protein. The rearrangement of the residues in the hydrophobic core of the mutant FALDH might be the likely reason behind the displacement of the transmembrane domain. The C-terminal alpha helix domain (Gly445-Asn460) is a unique structural feature of the human FALDH protein, which is not observed with any other soluble aldehyde dehydrogenases, that actively regulates the substrate gating process (Keller et al., 2014). The loss of conformational stability in the C-termini of the variants p.(Gly403Asp) and p.(Pro442Leu) might possess a direct impact on the dimerization of FALDH protein (Supp. Figure S5). A significant change in hydrophobicity of the C-terminal oligomerization domain was observed with the substitution of less hydropathic proline with more hydropathic leucine at the

This article is protected by copyright. All rights reserved.

Accepted Article

442nd amino acid position (Supp. Figure S6). This may affect the critical radius of the transit canal as observed with certain other voltage-gated channel proteins (Zhang et al., 2018), which might impair the substrate specific gating process in FALDH, thus causing SLS. The profound loss of FALDH activity by the clinical variants p.(Gly403Asp), p.(Pro442Leu) and p.(Trp450Ter) of FALDH strongly substantiates this conclusion. Previously, Rizzo et al., (1999) reported a homozygous p.(Lys447Glu) variant of FALDH in a SLS case with Japanese ethnicity that occurs in the C-terminal α helix. Exon-9 encodes the C-terminal α helix region of FALDH. Based on previous literature, there are 21 case reports of diverse clinical phenotypes in 35 SLS patients from Indian ethnicity, however only three disease-associated mutations in *ALDH3A2* have been documented including c.142G>T in exon-1 in siblings (Sakai et al., 2010) and a compound heterozygous c.126delG in exon-1 and c.529C>T in exon-4 of a 4-year-old boy (Nagappa et al., 2017). Epidermal dysfunctions resulted by the biochemical changes in SLS is quite complex. Functionally defective FALDH activity has been recorded in all the epidermal cells among the SLS cases. Diverse ichthyotic features were observed among SLS patients worldwide (Tanteles et al., 2015; Paige et al., 1994; Judge et al., 1990). Epidermal hyperplasia, hyperkeratosis mild intracellular edema spongiosis, hypergranulosis and a perivascular to interstitial infiltrate, and the presence of eosinophilic leaky epidermis and keratin containing milia like lipid vacuoles characterized the dermatological manifestations in our SLS patients. Moreover, the structural abnormalities in the skin due to the lack of aldehyde oxidizing activity were validated by histochemical staining of fresh skin biopsies with octanal as a substrate, which stains the epidermis of the normal skin darker. The results of histochemical staining of skin biopsies obtained from SLS cases who harboured p.(Gly403Asp) and p.(Glu67Ter) mutations

This article is protected by copyright. All rights reserved.

clearly evidenced less active FALDH activity in the epidermis than control and these observations corroborated with the findings as reported previously (Rizzo et al., 2010).

Despite the increasing recognition of SLS cases worldwide, therapeutic interventions appear to be limited. With personalised therapeutics slowly gearing up worldwide over the past decade, this study expanding the clinical spectrum and associated clinical mutations in *ALDH3A2*, which might help clinicians, patients and researchers in understanding the etiology, phenotypic features and therapy of intriguing disorders like SLS.

Acknowledgments

We thank all the patients and families for their cooperation throughout the study. RM was financially supported by Lady Tata Memorial Trust, Mumbai through a Junior Research Scholar Fellowship (No: LTMT-JRS/2018-20). Authors gratefully acknowledge Universities with Potential for Excellence (UPE), University Grants Commission- Special Assistance Programme (UGC-SAP) and Department of Science & Technology-Promotion of University Research and Scientific Excellence (DST-PURSE) programs of Madurai Kamaraj University for the infrastructure and other facilities. The authors report no targeted funding.

Data availability statement

All relevant data are within the paper, any additional information about the cohorts may be made available upon request addressed to the corresponding author, pending the approval of the Institutional Review Board of the Madurai Kamaraj University, Madurai.

This article is protected by copyright. All rights reserved.

Accepted Article

Accepted Article

Web Resources

- OMIM (https://www.omim.org/)
- NCBI (https://www.ncbi.nlm.nih.gov/nuccore)
- HGMD (http://www.hgmd.cf.ac.uk)
- The ALDH3A2 gene homepage in Leiden Open Variation Database (www.LOVD.nl/ALDH3A2)
- UCSC hg19 from UCSC genome Browser (https://genome.ucsc.edu/cgi-bin/hgGateway?db=hg19&redirect=manual&source=genome.ucsc.edu)
- Mutation Taster (http://www.mutationtaster.org/)
- MutPred (http://mutpred.mutdb.org/)
- PROVEAN (http://provean.jcvi.org/index.php)
- DynaMut (http://biosig.unimelb.edu.au/dynamut/)
- PredictSNP (https://loschmidt.chemi.muni.cz/predictsnp/)
- RNAfold (http://rna.tbi.univie.ac.at/cgi-bin/RNAWebSuite/RNAfold.cgi)
- MutaBind2 (https://lilab.jysw.suda.edu.cn/research/mutabind2/)
- I-TASSER (https://zhanglab.ccmb.med.umich.edu/I-TASSER/)
- CHARMM-GUI Membrane Builder (http://www.charmm-gui.org/?doc=input/membrane.bilayer)
- NEBcutter V2.0 (https://nc2.neb.com/NEBcutter2/)
- Human Phenotype Ontology (https://hpo.jax.org/app/)
- Exome Variant Server (http://evs.gs.washington.edu/EVS/)
- 1000 Genomes project database (http://www.1000genomes.org/)
- dbSNP (https://www.ncbi.nlm.nih.gov/snp/)
- Human Splicing Finder v3.1 (http://umd.be/HSF3/HSF.shtml)

Conflicts of interest

The authors declare no potential conflicts of interest with respect to the authorship and /or publication of this article.

This article is protected by copyright. All rights reserved.

Accepted Article

References

Bindu, P. S. (2020). Sjogren-Larsson Syndrome: Mechanisms and Management. *The Application of Clinical Genetics, 13,* 13. https://doi.org/10.2147/TACG.S193969.

Flore, L. A., & Milunsky, J. M. (2012). Updates in the genetic evaluation of the child with global developmental delay or intellectual disability. *Seminars in Pediatric Neurology 19*(4), 173-180. WB Saunders. https://doi.org/10.1016/j.spen.2012.09.004.

Fuijkschot, J., Maassen, B., Gorter, J. W., Gerven, M. V., & Willemsen, M. (2009). Speech-language performance in Sjögren-Larsson syndrome. *Developmental Neurorehabilitation, 12*(2), 106-112. https://doi.org/10.1080/17518420902800944.

Jagell, S., & Liden, S. (1982). Ichthyosis in the Sjögren-Larsson syndrome. *Clinical Genetics, 21*(4), 243-252. https://doi.org/10.1111/j.1399-0004.1982.tb00758.x.

Judge, M. R., Lake, B. D., Smith, V. V., Besley, G. T. N., & Harper, J. I. (1990). Depletion of alcohol (hexanol) dehydrogenase activity in the epidermis and jejunal mucosa in Sjögren-Larsson syndrome. *Journal of Investigative Dermatology, 95*(6), 632-634. https://doi.org/10.1111/1523-1747.ep12514294.

Keller, M. A., Zander, U., Fuchs, J. E., Kreutz, C., Watschinger, K., Mueller, T., Golderer, G., Liedl, K. R., Ralser, M., Kräutler, B., & Werner, E. R. (2014). A gatekeeper helix determines the substrate specificity of Sjögren-Larsson Syndrome enzyme fatty aldehyde dehydrogenase. *Nature Communications, 5*(1), 1-12. https://doi.org/10.1038/ncomms5439.

Kelson, T. L., McVoy, J. R. S., & Rizzo, W. B. (1997). Human liver fatty aldehyde dehydrogenase: microsomal localization, purification, and biochemical

This article is protected by copyright. All rights reserved.

Accepted Article

characterization. *Biochimica et Biophysica Acta (BBA)-General Subjects, 1335*(1-2), 99-110. https://doi.org/10.1016/s0304-4165(96)00126-2.

Lowry, O. H., Rosebrough, N. J., Farr, A. L., & Randall, R. J. (1951). Protein measurement with the Folin phenol reagent. *Journal of Biological Chemistry, 193*, 265-275. https://doi.org/10.1016/S0021-9258(19)52451-6.

Maia, M. (1974). Sjögren-Larsson syndrome in two sibs with peripheral nerve involvement and bisalbuminaemia. *Journal of Neurology, Neurosurgery & Psychiatry*, *37*(12), 1306-1315. https://dx.doi.org/10.1136/jnnp.37.12.1306.

Marchitti, S. A., Orlicky, D. J., Brocker, C., & Vasiliou, V. (2010). Aldehyde dehydrogenase 3B1 (*ALDH3B1*): immunohistochemical tissue distribution and cellular-specific localization in normal and cancerous human tissues. *Journal of Histochemistry & Cytochemistry, 58*(9), 765-783. https://doi.org/10.1369/jhc.2010.955773.

Mulder, J. D., & Landsmeer, J. M. F. (1968). The mechanism of claw finger. *The Journal of Bone and Joint Surgery, British volume, 50*(3), 664-668. https://doi.org/10.1302/0301-620X.50B3.664.

Nagappa, M., Bindu, P. S., Chiplunkar, S., Gupta, N., Sinha, S., Mathuranath, P. S., Bharath, R. D., & Taly, A. B. (2017). Child Neurology: Sjögren-Larsson syndrome. *Neurology, 88*(1), e1-e4. https://doi.org/10.1212/WNL.0000000000003456.

Paige, D. G., Morse-Fisher, N., & Harper, J. I. (1994). Quantification of stratum corneum ceramides and lipid envelope ceramides in the hereditary ichthyoses. *British Journal of Dermatology, 131*(1), 23-27. https://doi.org/10.1111/j.1365-2133.1994.tb08452.x.

This article is protected by copyright. All rights reserved.

Accepted Article

Rizzo, W. B. (2007). Sjögren-Larsson syndrome: molecular genetics and biochemical pathogenesis of fatty aldehyde dehydrogenase deficiency. *Molecular Genetics and Metabolism*, *90*(1), 1-9. https://doi.org/10.1016/j.ymgme.2006.08.006.

Rizzo, W. B., & Craft, D. A. (1991). Sjögren-Larsson syndrome. Deficient activity of the fatty aldehyde dehydrogenase component of fatty alcohol: NAD+ oxidoreductase in cultured fibroblasts. *The Journal of Clinical Investigation, 88*(5), 1643-1648. https://doi.org/10.1172/JCI115478.

Rizzo, W. B., Carney, G., & Lin, Z. (1999). The molecular basis of Sjögren-Larsson syndrome: mutation analysis of the fatty aldehyde dehydrogenase gene. *The American Journal of Human Genetics*, *65*(6), 1547-1560. https://doi.org/10.1086/302681.

Rizzo, W. B., Dammann, A. L., & Craft, D. A. (1988). Sjögren-Larsson syndrome. Impaired fatty alcohol oxidation in cultured fibroblasts due to deficient fatty alcohol: nicotinamide adenine dinucleotide oxidoreductase activity. *The Journal of Clinical Investigation, 81*(3), 738-744. https://doi.org/10.1172/JCI113379.

Rizzo, W. B., S'Aulis, D., Jennings, M. A., Crumrine, D. A., Williams, M. L., & Elias, P. M. (2010). Ichthyosis in Sjögren-Larsson syndrome reflects defective barrier function due to abnormal lamellar body structure and secretion. *Archives of Dermatological Research, 302*(6), 443-451. https://doi.org/10.1007/s00403-009-1022-y.

Rogers, G. R., Markova, N. G., De Laurenzi, V., Rizzo, W. B., & Compton, J. G. (1997). Genomic organization and expression of the human fatty aldehyde dehydrogenase gene (FALDH). *Genomics, 39*(2), 127-135. https://doi.org/10.1006/geno.1996.4501.

This article is protected by copyright. All rights reserved.

Accepted Article

Roy, U., Das, U., Pandit, A., & Debnath, A. (2016). Sjögren-Larsson syndrome: a rare disease of the skin and central nervous system. *BMJ Case Reports, 2016*, bcr2016215110. https://doi.org/10.1136/bcr-2016-215110.

Sakai, K., Akiyama, M., Yanagi, T., Nampoothiri, S., Mampilly, T., Sunitha, V., & Shimizu, H. (2010). Medical genetics: An Indian family with Sjögren-Larsson syndrome caused by a novel *ALDH3A2* mutation. *International Journal of Dermatology, 49*(9), 1031-1033. https://doi.org/10.1111/j.1365-4632.2010.04482.x.

Shapovalov, M. V., & Dunbrack Jr, R. L. (2011). A smoothed backbone-dependent rotamer library for proteins derived from adaptive kernel density estimates and regressions. *Structure, 19*(6), 844-858. https://doi.org/10.1016/j.str.2011.03.019.

Sjogren, T. (1957). Oligophrenia in combination with congenital ichthyosis and spastic disorders; a clinical and genetic study. *Acta Psychiatrica et Neurologica Scandinavica, 32*(133), 1-112. https://doi.org/10.1017/S1120962300019806.

Tanteles, G.A., Nicolaou, M., Patsia, N., Delikurt-Tuncalp, T., Spanou-Aristidou, E., Leonidou, E., Kyriakides, T. & Christophidou-Anastasiadou, V. (2015). A rare cause of pruritic ichthyosis: Sjögren-Larsson syndrome in the first reported patients of Cypriot descent. *European Journal of Dermatology, 25*(5), 495-496. https://www.jle.com/10.1684/ejd.2015.2615.

Weustenfeld, M., Eidelpes, R., Schmuth, M., Rizzo, W. B., Zschocke, J., & Keller, M. A. (2019). Genotype and phenotype variability in Sjögren-Larsson syndrome. *Human Mutation, 40*(2), 177-186. https://doi.org/10.1002/humu.23679.

This article is protected by copyright. All rights reserved.

Accepted Article

Willemsen, M. A. A. P., Rotteveel, J. J., Van Domburg, P. H. M. F., Gabreëls, F. J. M., Mayatepek, E., & Sengers, R. C. A. (1999). Preterm birth in Sjögren-Larsson syndrome. *Neuropediatrics, 30*(06), 325-327. https://doi.org/10.1055/s-2007-973513.

Zhang, X. C., Yang, H., Liu, Z., & Sun, F. (2018). Thermodynamics of voltage-gated ion channels. *Biophysics Reports, 4*(6), 300-319. https://doi.org/10.1007/s41048-018-0074-y.

Zheng, L., Baumann, U., & Reymond, J. L. (2004). An efficient one-step site-directed and site-saturation mutagenesis protocol. *Nucleic Acids Research, 32*(14), e115. https://doi.org/10.1093/nar/gnh110.

This article is protected by copyright. All rights reserved.

Accepted Article

Figure Legends:

Figure 1. **Clinical manifestations of SLS cases**. A) Case-1; B) Case-2; C) Case-3; D) Case-4; E) Case-5 F) Case-6. A red star depicts the presence of novel phenotype-

This article is protected by copyright. All rights reserved.

Accepted Article

"intrinsic-minus-claw hands" in case-5 & -6 from same family. All patients have spastic diplegia, except case-5 & -6 with quadriparesis.

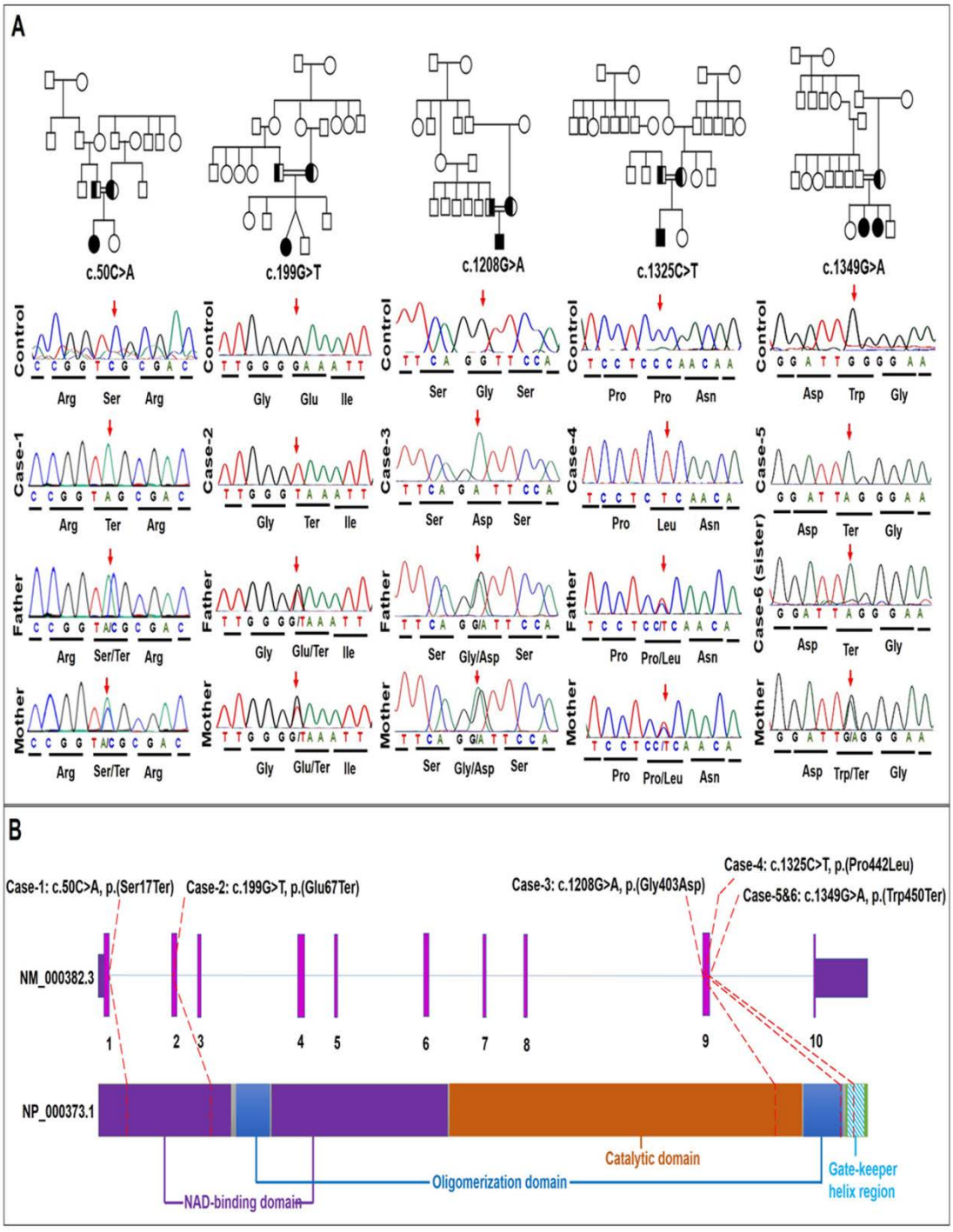

Figure 2. Pedigree and portion of electropherograms depicting pattern of inheritance and localization of variants. A) Family pedigree and DNA sequence chromatograms of SLS cases and their families. All the probands were homozygous

This article is protected by copyright. All rights reserved.

and their parents were heterozygous for the identified clinical variants in *ALDH3A2* gene substantiating autosomal recessive mode of inheritance. B) Schematic diagram of *ALDH3A2* gene, protein structure of FALDH and variants detected in this study. Gene structure with exons and introns shows the location of the identified variants. The protein structure highlights the NAD binding domain in violet, catalytic domain in brown, oligomerization domain in dark blue and the gatekeeper domain in light blue shades.

Accepted Article

This article is protected by copyright. All rights reserved.

Accepted Article

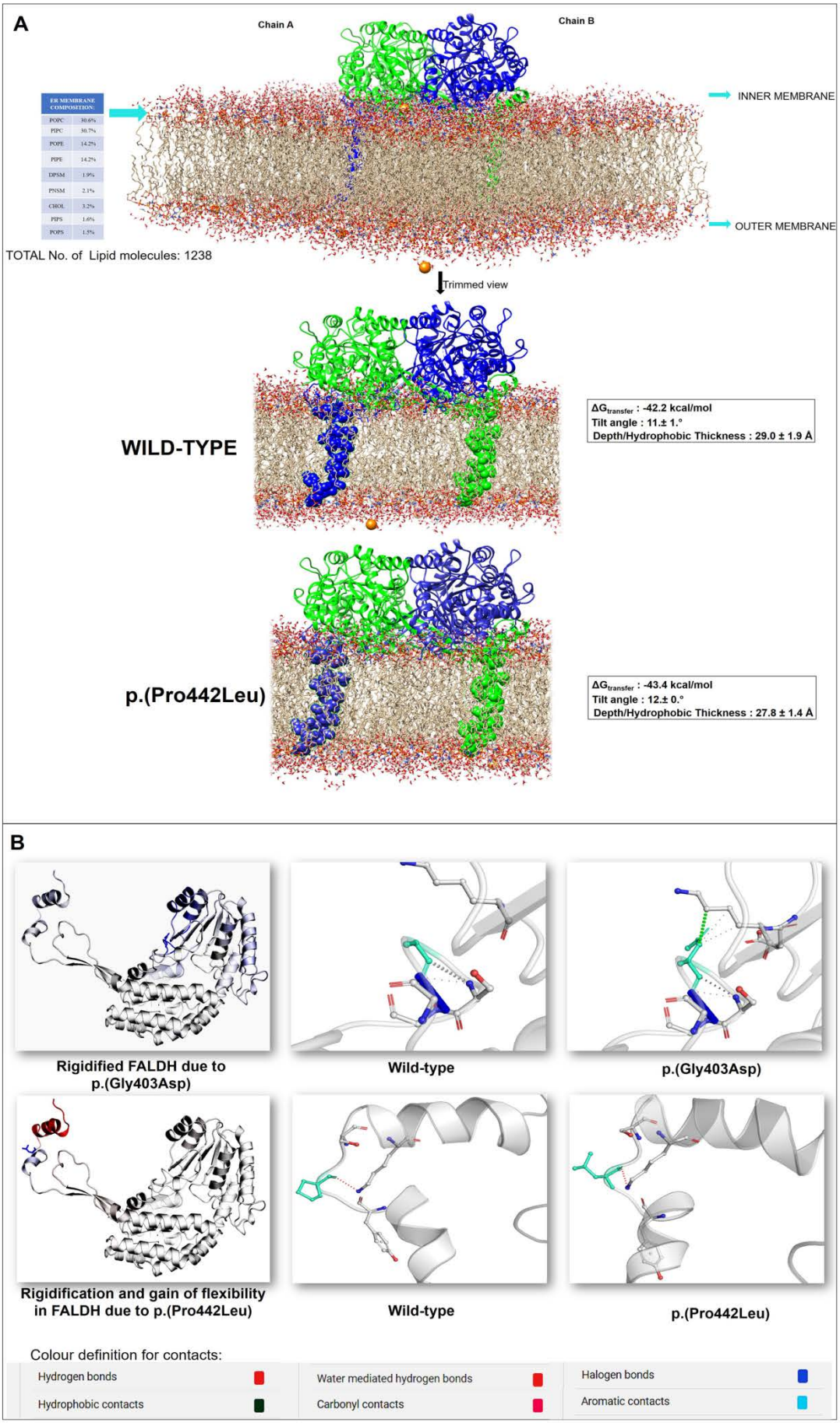

This article is protected by copyright. All rights reserved.

Accepted Article

Figure 3. **Predicting mechanism of pathogenesis.** A) Orientation of the FALDH wild-type and mutants depicting the change in conformation of protein structure. Displacement of the structural components like transmembrane domain has been observed with p.(Pro442Leu), which might attribute for the functional impairment of FALDH enzyme (Abbreviations: POPC- 1-Palmitoyl-2-oleoyl-sn-glycero-3-phosphocholine; PIPC - phosphatidylcholine (PC) lipid corresponding to atomistic e.g. C16:0/18:2 1-palmitoyl-2-linoleoyl tails; POPE- 1-Palmitoyl-2-oleoyl-sn-glycero-3-phosphoethanolamine; PIPE - piperazine-N,N′-bis(2-ethanesulfonic acid; DPSM-dipalmitoyl sphingomyelin; PNSM- sphingomyelin (SM) lipid corresponding to atomistic e.g. C(d18:1/24:1) tails; CHOL- Cholesterol; PIPS- Phosphatidylinositol (3,4,5)-trisphosphate; POPS- 1-palmitoyl-2-oleoyl-sn-glycero-3-phosphoserine); B) Vibrational entropy predictions and deformation analysis for p.(Gly403Asp) and p.(Pro442Leu): Interatomic interactions of wild-type and the missense mutants in the region of C-terminal alpha helix with p.(Gly403Asp) and p.(Pro442Leu) variants shows gain or loss of flexibility of the mutant FALDH.

This article is protected by copyright. All rights reserved.

Accepted Article

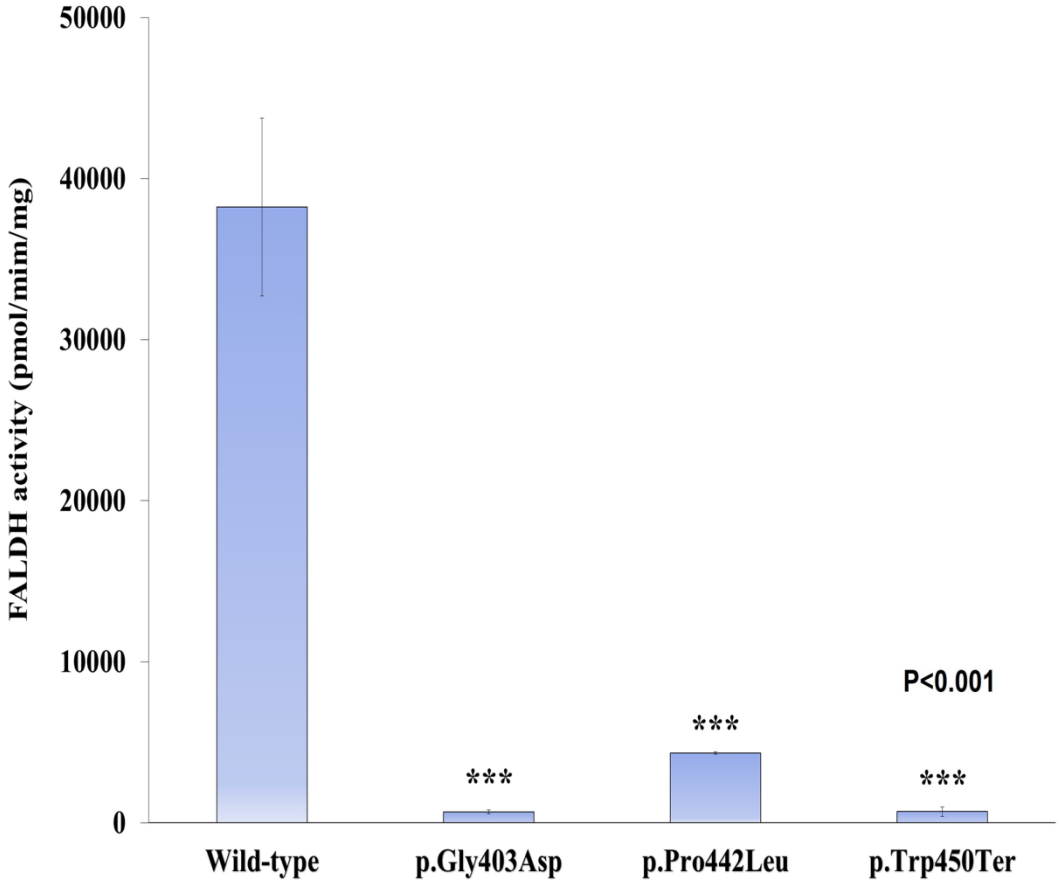

Figure 4. **Functional characterization of clinical mutants by FALDH assay.** NAD^+-dependent aldehyde dehydrogenase activity assay with octadecanal substrate depicting highly significant reduction of enzyme activity for the FALDH mutants p.Gly403Asp, p.(Pro442Leu) and p.(Trp450Ter) with *P* value = 0.0003, 0.0004 and 0.0003, respectively.

This article is protected by copyright. All rights reserved.

Accepted Article

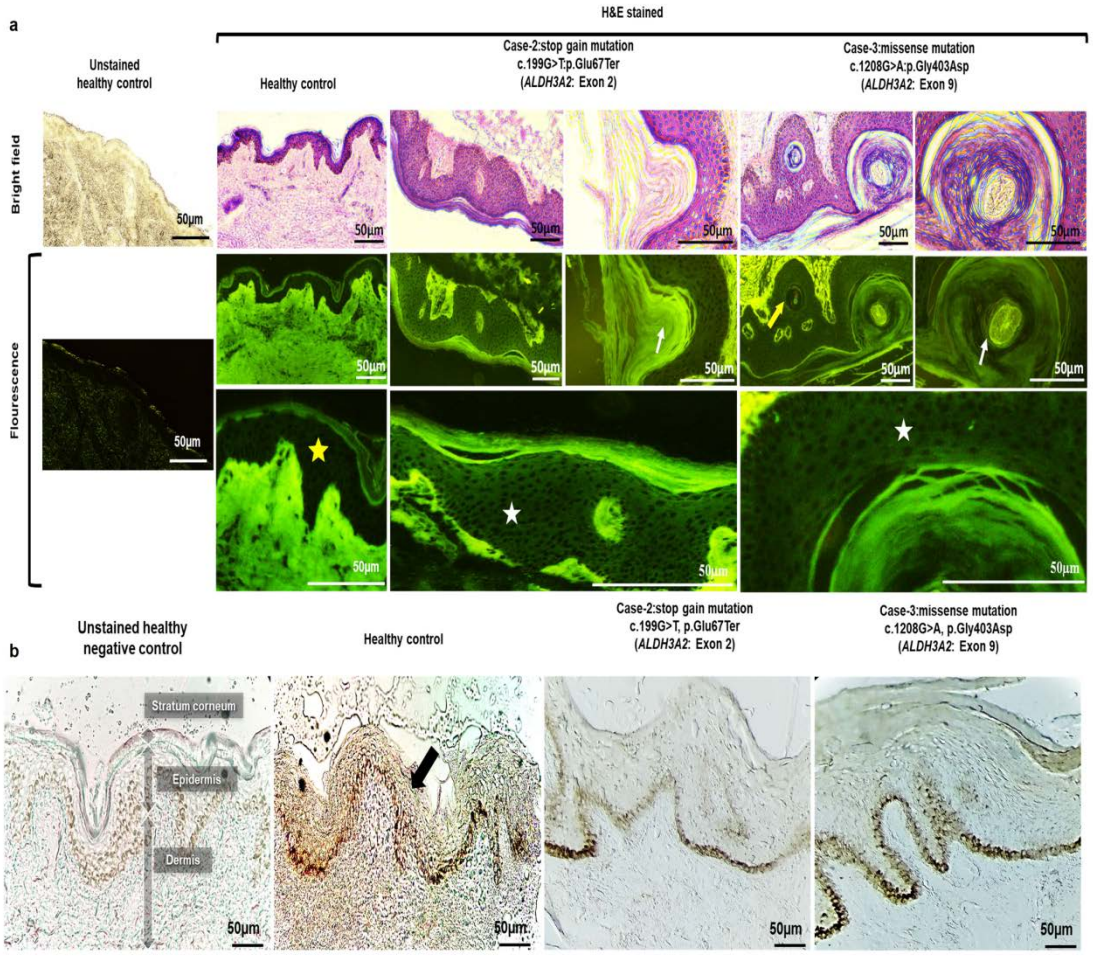

Figure 5. Cutaneous pathogenesis of clinical variants p.(Gly403Asp) and p.(Glu67Ter). (A) H&E staining of rectus femoris 12 µm cryostat tissue sections revealed epidermal hyperplasia with mild intracellular edema spongiosis, hypergranulosis and perivascular to interstitial lymphocytic infiltration with p.(Gly403Asp) and p.(Glu67Ter). Eosin stained dermis region reveals leaky epidermis. Fluorescent imaging of H&E stained tissue sections uncovered the diffusion of eosin in to epidermis attributing to its leaky nature (yellow star corresponds to hematoxylin stained non-fluorescent intact epidermis while white star corresponds to eosin diffused fluorescent leaky epidermis). Keratin containing milia like lipid vacuoles are observed with p.(Gly403Asp) and p.(Glu67Ter). Yellow arrow indicates the presence of keratin containing hair follicle, while white arrow indicates

This article is protected by copyright. All rights reserved.

the presence of lipid vacuoles encompassing a different fluorescent core region which is different from a hair follicle. (B) Histochemical staining for aldehyde oxidizing activity in normal and SLS skin biopsies. Pale histochemical staining in p.(Gly403Asp) and p.(Glu67Ter) when compared to healthy control tissue sections implies reduced aldehyde oxidizing activity in these mutants.

Table 1. Edgotype datasheet - correlation between the genotype and phenotype of all 6 SLS cases describing their clinical and mutational profile.

Parameter	**C1**	**M1**	**Case-1**	**Case-2**	**Case-3**	**Case-4**	**Case-5**	**Case-6**
Age (yrs)	**28**	**40**	**5**	**3**	**16**	**8**	**12**	**13**
Sex (F/M)	**F**	**F**	**F**	**F**	**M**	**M**	**F**	**F**
Weight (kg)	**68**	**80**	**8.5**	**9**	**33.2**	**10**	**7.3**	**10.25**
Circumference of head (cms)	**50**	**52**	**43**	**42**	**52**	**48**	**45**	**46**
Preterm (PT)/term (T)	**T**	**T**	**T**	**PT**	**PT**	**PT**	**PT**	**PT**
Developmental phenotypes								
Global developmental delay	-	-	+	+	+	+	+	+
Intellectual disability (IQ[a])	**- (120)**	**- (100)**	**+ (50)**	**+ (40)**	**+ (70)**	**+ (50)**	**+ (40)**	**+ (30)**
Neurological phenotypes								
Epilepsy MRI findings	-	-	-	-	+	-	-	-
Periventricular white matter changes	-	-	-	+	-	-	+	+
T2 hyperintense lesions	-	-	-	-	-	+	-	-
Behavioural phenotypes								

This article is protected by copyright. All rights reserved.

Accepted Article

Accepted Article

Autistic behaviour	-	-	-	-	-	+	-	-
Hyperactivity	-	-	-	-	-	+	-	-
Muscular phenotypes								
Exaggerated reflexes	-	-	+	-	-	-	-	-
Increased muscle tone	-	-	-	-	-	-	+	+
Decreased muscle tone	-	-	+	-	-	-	-	-
Claw hand	-	-	-	-	-	-	+	+
Spastic quadriparesis	-	-	-	-	-	-	+	+
Spastic diplegia	-	-	+	+	+	+	-	-
Abnormal walk	-	-	-	-	-	-	-	+
Ichthyosis related phenotypes								
Collodion baby	-	-	-	+	+	+	+	+
Ichthyosis	-	-	+	+	+	+	+	+
Periventricular pits	-	-	+	-	-	-	-	-
Other rare phenotypes								
End gaze nystagmus	-	-	+	-	-	-	-	-
Loss of speech	-	-	+	+	-	+	+	+
Low-set ears	-	-	+	-	-	-	-	-
Small tragus	-	-	+	-	-	-	-	-
Hypertelorism	-	-	+	-	-	-	-	-
Genotype								
Mutation	-	c.1349 G>A: p.(Trp450Ter)	c.50 C>A: p.(Ser17Ter)	c.199 G>T: p.(Glu67Ter)	c.1208 G>A: p.(Gly403Asp)	c.1325 C>T: p.(Pro442Leu)	c.1349 G>A: p.(Trp450Ter)	c.1349 G>A: p.(Trp450Ter)

This article is protected by copyright. All rights reserved.

Status	-	Heterozygous	Homozygous	Homozygous	Homozygous	Homozygous	Homozygous	Homozygous

[a] Intellectual Quotient (IQ) - Calculated based on cumulative scores of various scales of intellectual functioning and adaptive behaviour adapted for Indian population. C1- Unrelated healthy control and M1- Carrier mother of SLS case-5 & 6.

Table 2. Mutational pathogenicity analysis *in silico*.

c.50C>A:p.(Ser17Ter) (ch17:19649021, C→A) (Exonic) (Stop-gain)							
Software	Mutation Taster	MutPred	Provean	PredictSNP	SIFT	PolyPhen	FATHMM
Prediction	Disease causing	NA	NA	NA	NA	NA	Deleterious
Score	1.00	-	-	-	-	-	0.8138
c.199G>T:p.(Glu67Ter) (ch17:19651592,G→T) (Exonic) (Stop-gain)							
Software	Mutation Taster	MutPred	Provean	PredictSNP	SIFT	PolyPhen	FATHMM
Prediction	Disease causing	NA	NA	NA	NA	NA	Deleterious
Score	0.99	-	-	-	-	-	0.9969
c.1208G>A:p.(Gly403Asp) (ch17:19671721, G→A) (Exonic) (Missense)							
Software	Mutation Taster	MutPred	Provean	PredictSNP	SIFT	PolyPhen	FATHMM
Prediction	Disease causing	Loss of catalytic site at S405, Altered transmembrane domain and metal binding	Deleterious	Deleterious	Deleterious	Probably damaging	Deleterious
Score	0.99	0.946	-6.714	87%	53%	0.97	0.9482
c.1325C>T:p.(Pro442Leu) (ch17:19671838, C→T) (Exonic) (Missense)							
Software	Mutation Taster	MutPred	Provean	PredictSNP	SIFT	PolyPhen	FATHMM
Prediction	Disease	Loss of B-factor, Loss	Deleterious	Deleterious	Deleterious	Probably	Deleterious

This article is protected by copyright. All rights reserved.

Accepted Article

	causing	of acetylation at K437				damaging	
Score	0.99	0.878	-9.428	87%	79%	1.0	0.9409
c.1349G>A:p.(Trp450Ter) (ch17:19671862, G→A) (Exonic) (Stop-gain)							
Software	Mutation Taster	MutPred	Provean	PredictSNP	SIFT	PolyPhen	FATHMM
Prediction	Disease causing	NA	NA	NA	NA	NA	Deleterious
Score	1.0	-	-	-	-	-	0.9465

Accepted Article

This article is protected by copyright. All rights reserved.